INVESTIGATION OF HARD TARGETS FOR CALIBRATION OF A COHERENT DOPPLER LIDAR SYSTEM

by

Richard Anderson
Professor of Physics
University of Missouri-Rolla
Rolla, Missouri

ABSTRACT

The bihemispherical reflectance has been measured for a diffuse gold surface the same as the coating on the integrating sphere, flowers of sulfur, sandblasted aluminum, and 120 grade aluminum oxide sandpaper. The sandpaper measurements indicate that materials with low reflectance cannot be measured until more sensitive detection techniques are found. The sphere had to be used without a detector baffle so an unusual geometry was needed that led to a loss of intensity. Further, it is estimated that some first-strike light entered the detector and the readings could be 1 to 1.5% too low. A limited number of normal incident directional-hemispherical reflectance measurements were made on aluminum and sandpaper. Several recommendations are made which are: (1) the proper baffle placement; (2) improve lock-in detection using a PAR lock-in amplifier or the heterodyne technique; (3) modification of the sphere so the sample may be mounted at the cell center on a graduate, rotatable table for measurement of directional-hemispherical reflectance; (4) the purchase of additional diffuse gold samples with coatings like the sphere; and (5) better laser temperature control to improve intensity stability.

ACKNOWLEDGEMENTS

I am honored to be selected by James W. Bilbro to participate in the Summer Faculty Fellowship Program. James Bilbro and William Jones must be thanked for having assembled the necessary equipment. I appreciate the opportunity to work on this project for it expands my experience base in optics and this will be helpful in both my research and teaching.

Steve Johnson must be thanked for answering all my questions about the laboratory, his research project, and for locating special equipment. In order to keep all the equipment in operation, I am indebted to Al Kosis. Bob Rood must be thanked for machining and sandblasting my samples and sample holder. Finally, this report could not have been written without the excellent typing of the program secretary.

LIST OF FIGURES

Figure number	Title	Page
1	Lay-out for uniform irradiation of sample.	10
2	Lay-out for direct irradiation of sample.	10
3	Dual beam measurement technique.	11
4	Edward's Method.	11
5	Uniform irradiation problem.	16
6	Direct irradiation problem.	16
7	Correct baffle position.	17
8	Small irradiation angle.	17

LIST OF TABLES

Table Number	Title	Page
1	Reflectance of diffuse gold, sand-blasted aluminum, 120 grade aluminum oxide sandpaper, and flowers of sulfur.	19
2	Maximun deviation in a typical reading produced by $\pm 2\mu W$ detector signal variation.	20
3	The effect of sample orientation on the reflectance of sulfur.	21
4	Sulfur reflectance for three lines for fixed and random sample orientations.	22
5	Normal incident directional-reflectance, $\rho(2\pi)$, of aluminum and 120 grade aluminum oxide sandpaper.	24
6	Summary of diffuse gold wall coating reflectance.	25

INTRODUCTION

The reflectance of durable hard target samples is needed to calibrate a lidar system. The knowledge of the backscattering coefficient of a hard target, $\rho^*(\pi)$, is required for the calibration of the efficiency of the system to be used where radiation has been backscattered from diffuse targets. The backscattering coefficient, $\rho^*(\pi)$, has the units of steradians^{-1} and is defined as the ratio of the power per steradian backscattered toward the transmitter-receiver to the incident power. The backscatter coefficient is related to the reflectance of the hard target. This relation is seen by defining the bidirectional reflectance distribution function (BRDF) of the target. The BRDF is the ratio of the reflected radiance $dL_r(\theta_i, \phi_i; \theta_r, \phi_r; \lambda_i)$ (W m^{-2} sr^{-1}) confined in a solid angle element $d\omega_r$ in the direction (θ_r, ϕ_r) and the incident irradiance in the solid angle element $d\omega_i$ in the direction (θ_i, ϕ_i).

$$\text{BRDF} = f_r(\theta_i,\phi_i;\ \theta_r,\phi_r) = \frac{dL_r(\theta_i,\phi_i;\ \theta_r,\phi_r;\ \lambda_i)}{L_i(\theta_i,\phi_i)\ \text{Cos}\ \theta_i\ d\omega_i} \quad (1)$$

It is noted the L_r is dependent both on the incident beam's wavelength and polarization. The most general reflectance is the biconical reflectance and is defined as the ratio of the reflected to the incident flux where reflected flux, ϕ_r, is given by,

$$\phi_r = dA \int_{\omega_r} L_r(\theta_r,\phi_r)\ \text{Cos}\ \theta_r\ d\omega_r$$

$$= dA \int_{\omega_i} \int_{\omega_r} dL_r(\theta_i,\phi_i;\ \theta_r,\phi_r;\lambda_i)\ \text{Cos}\ \theta_r\ d\omega_r$$

and the incident flux, ϕ_i, is

$$\phi_i = dA \int_{\omega_i} L_i(\theta_i,\phi_i)\ \text{Cos}\ \theta_i\ d\omega_i$$

so

$$\rho(\theta_i,\phi_i;\theta_r,\phi_r) = \frac{\int_{\omega_i}\int_{\omega_r} f_r(\theta_i,\phi_i;\theta_r,\phi_r)L_i(\theta_i,\phi_i)\ \text{Cos}\ \theta_i\ \text{Cos}\ \phi_r\ d\omega_i\ d\omega_r}{\int_{\omega_i} L_i(\theta_i,\phi_i)\ \text{Cos}\ \theta_i\ d\omega_i}$$

If the incident flux is uniform and isotropic $L_i\ (\theta_i,\phi_i)$ is constant and the reflectance becomes

$$\rho(\theta_i,\phi_i;\theta_r,\phi_r) = \frac{\int_{\omega_i}\int_{\omega_r} f_r(\theta_i,\phi_i;\theta_r,\phi_r)\cos\theta_i\cos\theta_r\, d\omega_i d\omega_r}{\int_{\omega_i}\cos\theta_i\, d\omega_i} \quad (2)$$

In the hard target calibration the target is irradiated from the direction (θ_i,ϕ_i) and radiates uniformly in the 2π steradian solid angle, so the reflectance of interest in lidar calibration is the directional-hemispherical reflectance $\rho(\theta_i,\phi_i;\ 2\pi)$ or

$$\rho(\theta_i,\phi_i;\ 2\pi) = \int_0^{2\pi}\int_0^{\pi/2} f_r(\theta_i,\phi_i;\theta_r,\phi_r)\cos\theta_r\sin\theta_r\, d\theta_r\, d\phi_r \quad (3)$$

where the solid angle ω_i is small and constant in this application.

The backscatter coefficient is defined by the equation

$$\rho^*(\omega_i,\omega_r) = \frac{\int_{\omega_i}\int_{\omega_r} f_r(\theta_i,\phi_i;\theta_r,\phi_r)\cos\theta_i\cos\theta_r\, d\omega_i\, d\omega_r}{\omega_r\int_{\omega_i}\cos\theta_i\, d\omega_i} \quad (4)$$

In the case of directional irradiation for the lidar system ω_i is small and constant and if the target is perfectly diffusing (Lambertian) or at least reproducible

$$\rho^*(\theta_i,\phi_i;2\pi) = \langle f_r(\theta_i,\phi_i;\theta_r,\phi_r)\rangle \cos\theta_r$$

where $\rho^*(\theta_i,\phi_i;\ 2\pi)$ is the directional -hemispherical coefficient and $\langle f_r(\theta_i,\phi_i;\ \theta_r,\phi_r)\rangle$ is the average value of f_r over the solid angle ω_r. For the backscatter coefficient $\rho^*(\pi)$, $\theta_r = 0$

$$\text{so}\quad \rho^*(\pi) = \langle f_r\ (\theta_i,\phi_i;\theta_r,\phi_r)\rangle \quad (5)$$

For a perfectly diffusing reflector (Lambertian)

$$f_r = f_{r,d} = \langle f_r\rangle = \text{constant}$$

and

$$\rho_d\ (\theta_i,\phi_i;2\pi) = L_{r,d}\, dA\int_{\omega_r}\cos\theta_r d\omega_r / E_i\, dA = f_{r,d}\int_{\omega_r}\cos\theta_r d\omega_r = f_{r,d}\,\pi$$

or $\langle f_r(\theta_i,\phi_i;\theta_r,\phi_r) \rangle = f_{r,d} = \rho(\theta_i,\phi_i;2\pi)/\pi = \rho(\omega_i;2\pi)/\pi$
and for an incident angle θ

$$\langle f_r(\theta_i,\phi_i;\theta_r,\phi_r)\rangle = \rho(\theta_i,\phi_i;2\pi)\text{Cos }\theta/\pi = \rho(\omega_i,2\pi)\text{Cos }\theta/\pi \quad (6)$$

The backscatter coefficient in these two cases is related to the reflectance as

$$\rho^*(\pi) = \rho(\theta_i,\phi_i;\ 2\pi)/\pi = \rho(\omega_i,\ 2\pi)/\pi$$

or (7)

$$\rho^*(\pi) = \rho(\theta_i,\phi_i;\ 2\pi)\text{Cos }\theta/\pi = \rho(\omega_i,2\pi)\ \text{Cos }\theta/\pi$$

Thus the directional reflectance is necessary to evalute $\rho^*(\pi)$.

A knowledge of the backscatter coefficient of the hard targets allows the determination of the minimum volume backscatter coefficient $\beta(\pi)_{min}$ of the atmosphere that can be detected which is a measure of the system's sensitivity. If the atmosphere can be modeled, the backscattering coefficient $\beta(\pi)$ of the atmosphere can be measured in terms of the known values of $\rho^*(\pi)$, the ratio of instrument overlap functions, and the ratio of the atmospheric absorption over the atmospheric and target paths.

An on-site calibration facility will allow one to study aging effects of hard targets and measure the reflectance of new candidates.

OBJECTIVES

The objective of this research will be to measure in the 9 and 10 μm CO_2 laser regions the reflectance of :

1. The diffuse gold coating of the integrating sphere, ρ_ω;

2. The reflectance versus polarizaton of various hard target samples under uniform irradiation which is the bihemispherical reflectance, $\rho(2\pi,2\pi)$;

3. The normal incidence directional-hemispherical reflectance of the samples versus polarization, $\rho(2\pi)$; and

4. The arbitrary directional-hemspherical reflectance versus polarization, $\rho(\theta,0;2\pi)$ where the sample is irradiated at various angles of incidence θ .

THEORY OF MEASUREMENTS

A. General Theory

The general theory for the reflectance of a sample in an integrating sphere will be derived. The interior of the sphere has a reflectance, ρ_ω, and it contains "n+1" elemental areas of different reflectances, ρ_n. The total surface area of the sphere, including the elements is A and each elemental area has an area, a_n, with a fractional area, $f_n = a_n/A$. The input flux to the sphere, ϕ_o is constant and the detector does not observe light scattered from the first strike.

The flux is incident upon an area, a_o , so the amount reflected is

$$\rho_o \phi_o \tag{8}$$

the amount incident on the ith area a_i is

$$f_i \rho_o \phi_o \tag{9}$$

and the amount incident upon the perfectly diffusing sphere wall of area $A - \sum_i a_i$ is

$$(1 - \sum_{i=0}^{n} f_i) \rho_o \phi_o \tag{10}$$

The amount reflected from the ith area is

$$\rho_i f_i \rho_o \phi_o \tag{11}$$

and from all the elemental areas is

$$\sum_{i=0}^{n} \rho_i f_i \rho_o \phi_o \tag{12}$$

The amount reflected from the perfectly diffusing walls of the integrating sphere is

$$\rho_\omega(1 - \sum_{i=0}^{n} f_i) \rho_o \phi_o \tag{13}$$

Then the total unabsorbed flux after the second reflection is

$$\rho_o\phi_o \{\rho_\omega(1 - \sum_{i=0}^{n} f_i) + \sum_{i=0}^{n} \rho_i f_i\} \tag{14}$$

and the sphere can be assigned an average reflectance $\bar{\rho}_\omega$, where

$$\bar{\rho}_\omega = \rho_\omega (1 - \sum_{i=0}^{n} f_i) + \sum_{i=0}^{n} \rho_i f_i \tag{15}$$

An amount of this reflected flux incident on the "n+1" elemental areas is

$$\sum_{i=0}^{n} f_i \, \bar{\rho}_\omega \, \rho_o \, \phi_o \tag{16}$$

and

$$(1 - \sum_{i=0} f_i) \, \bar{\rho}_\omega \, \rho_o \phi_o \tag{17}$$

is incident on the perfectly diffusing sphere surface. An amount reflected from the elemental areas is

$$\sum_{i=0}^{n} \rho_i \, f_i \, \bar{\rho}_\omega \, \rho_o \phi_o \tag{18}$$

and that reflected by the integrating sphere is

$$\rho_\omega \, (1 - \sum_{i=0}^{n} f_i) \, \bar{\rho}_\omega \, \rho_o \phi_o \tag{19}$$

The total unabsorbed flux after the third reflection is

$$\{\rho_\omega \, (1 - \sum_{i=0}^{n} f_i) + \sum_{i=0}^{n} \rho_i \, f_i\} \, \bar{\rho}_\omega \, \rho_o \phi_o \tag{20}$$

or it is

$$\bar{\rho}_\omega^2 \, \rho_o \phi_o \tag{21}$$

After n reflections the flux incident on the ith area is

$$\phi_i = f_i \, \rho_o \phi_o + f_i \, \bar{\rho}_\omega \, \rho_o \phi_o + f_i \, \bar{\rho}_\omega^2 \, \rho_o \phi_o + f_i \, \bar{\rho}_\omega^3 \, \rho_o \phi + \ldots$$

$$= f_i \, \rho_o \phi_o \, (1 + \bar{\rho}_\omega + \bar{\rho}_\omega^2 + \bar{\rho}_\omega^3 + \ldots + \bar{\rho}_\omega^{n-1}) \tag{22}$$

If the sphere is perfectly reflecting, the number of reflections approaches infinity and the sum becomes an infinite sum, so

$$\phi_i = f_i \, \rho_o \phi_o \, (1 + \bar{\rho}_\omega + \bar{\rho}_\omega^2 + \bar{\rho}_\omega^3 + \ldots)$$

$$= f_i \, \rho_o \phi_o / (1 - \bar{\rho}_\omega) \tag{23}$$

If the ith area is the emergent port, the total throughput of the sphere is the ratio of the emergent flux to the incident flux, so

$$\tau = \phi_m/\phi_o = f_m \rho_o/(1-\bar{\rho}_\omega) \quad (24)$$

where, f_m, is the fractional area of the emergent (detector) port.

For a general ith elemental area this same ratio is defined as the fraction of incident radiance on that area or

$$F_i = \phi_i/\phi_o = f_i \rho_o/(1-\bar{\rho}_\omega) \quad (25)$$

It is this equation that will be applied to the three different measurements to be performed in this experiment. More detailed theory is given in the references.

B. Uniform Irradiation of Sample (Substitution Method)

In order to measure $\rho(2\pi, 2\pi)$ the radiation must be incident upon the wall of the integrating sphere so that no first strike scattered radiation can reach the detector. In this case $\rho_o=\rho_\omega$ and the emergent flux is

$$\phi_m = f_m \rho_\omega \phi_o/(1-\bar{\rho}_\omega) \quad (26)$$

This irradiation technique is shown in Figure 6. The sphere used in our experiment has three ports or elemental areas; entrance of fractional area, f_e, emergent of fractional area, f_m, and sample of fractional area, f_s. Then equation (26) becomes

$$\phi_m = f_m \rho_\omega \phi_o/\{1-\rho_\omega (1-f_e-f_m-f_s) - \rho_s f_s\} \quad (27)$$

A knowledge of ρ_ω is required and can be determined by using (1) the diffuse gold sample and (2) no sample in the sample port, so the reflectances of the two samples are $\rho_s=\rho_\omega$ and $\rho_s=0$, respectively. In the two cases ϕ_m becomes

$$\phi_{m_\omega} = f_m \rho_\omega \phi_o/\{1-\rho_\omega(1-f_e-f_m)\} \quad (28)$$

and

$$\phi_{m_o} = f_m \rho_\omega \phi_o/\{1-\rho_\omega(1-f_e-f_m-f_s)\} \quad (29)$$

Let

$$\alpha_1 = (1 - f_e - f_m) \tag{30}$$

and

$$\alpha_2 = (1 - f_e - f_m - f_s) \tag{31}$$

so

$$\phi_{m_\omega} = f_m \rho_\omega \phi_o/(1-\rho_\omega \alpha_1) \tag{32}$$

and

$$\phi_{m_o} = f_m \rho_\omega \phi_o/(1-\rho_\omega \alpha_2) \tag{33}$$

The signals are porportional to

$$S_\omega = K \phi_{m_\omega} \tag{34}$$

and

$$S_o = K \phi_{m_o} \tag{35}$$

and on multiplying equations (32) and (33) by K and solving for $K f_m \rho_\omega \phi_o$, then

$$S_{m_\omega} (1 - \rho_\omega \alpha_1) = S_{m_o} (1 - \rho_\omega \alpha_2) \tag{36}$$

Let

$$\beta = S_{m_\omega}/S_{m_o} \tag{37}$$

Then

$$\rho_\omega = (\beta-1)/(\beta \alpha_1-\alpha_2) \tag{38}$$

If the reflectance of the integrating sphere is accurately measured, the reflectance of samples may be measured. Again the wall of the integrating sphere is irradiated, so the sample is uniformly irradiated and the measurements of signal are made with and without the sample, so the emergent fluxes are with the sample

$$\begin{aligned} \phi_{m_s} &= f_m \rho_\omega \phi_o/\{1 - \rho_\omega (1 - f_e-f_m-f_s) - \rho_s f_s\} \\ &= f_m \rho_\omega \phi_o/\{1 - \rho_\omega \alpha_2 - \rho_s f_s\} \end{aligned} \tag{39}$$

and without a sample

$$\begin{aligned} \phi_{m_o} &= f_m \rho_\omega \phi_o/\{1-\rho_\omega(1-f_e-f_m-f_s)\} \\ &= f_m \rho_\omega \phi_o/\{1 - \rho_\omega \alpha_2\} \end{aligned} \tag{40}$$

Let the ratio of the signals be

$$\beta = S_{m_s}/S_{m_o} \tag{41}$$

then similar to the above case

$$\rho_s = (1 - \frac{1}{\beta}) \frac{(1-\rho_\omega \alpha_2)}{f_s} \tag{42}$$

C. Normal Irradiance of the Sample

In this type of irradiance either substitution of samples, a dual beam, or Edward's method may be used. These three techniques are seen in Figures 2,3, and 4.

In the substitution method the incident, nearly parallel beam of laser radiation is incident normally on the sample. The diffuse gold sample and target sample are alternately irradiated in the port and the output fluxes are

$$\phi_{m_\omega} = f_m \rho_\omega \phi_o / \{1-\rho_\omega(1-f_e-f_m)\} = f_m \rho_\omega \phi_o / \{1-\rho_\omega \alpha_1\} \tag{43}$$

and

$$\phi_{m_s} = f_m \rho_s \phi_o / \{1-\rho_\omega(1-f_e-f_m-f_s)-\rho_s f_s\} = f_m \rho_s \phi_o / (1-\rho_\omega \alpha_2 - \rho_s f_s) \tag{44}$$

The signals are $K\ \phi_{m_\omega}$ and $K\ \phi_{m_s}$, solving both equations for $K\ f_m\ \phi_o$ one has

$$\frac{S_{m_\omega}}{\rho_\omega}(1 - \rho_\omega\ \alpha_1) = \frac{S_{m_s}}{\rho_s}(1 - \rho_\omega\ \alpha_2 - f_s\ \rho_s) \tag{45}$$

Let

$$\beta = S_{m_\omega}/S_{m_s} \tag{46}$$

then

$$\rho_s(2\pi) = \rho_\omega\ (1-\rho_\omega\ \alpha_1)/\beta(1-\rho_\omega\ \alpha_2) \tag{47}$$

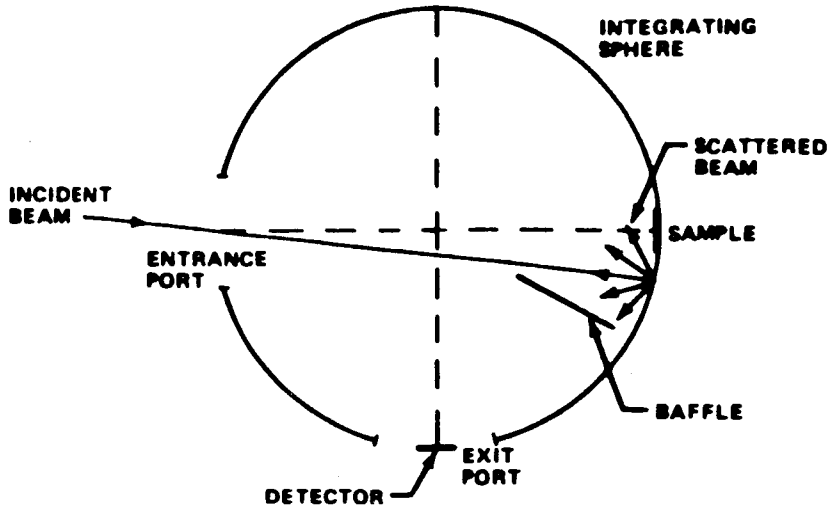

Figure 1. Lay-out for uniform irradiation of sample

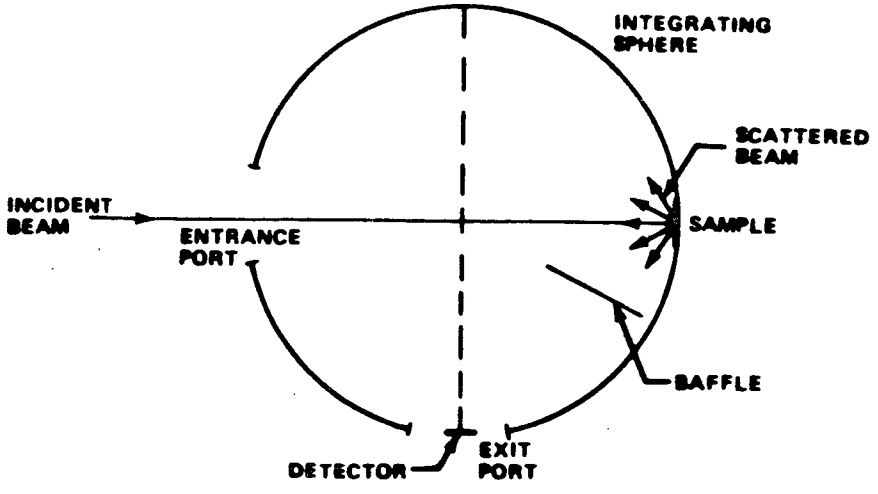

Figure 2. Lay-out for direct irradiation of sample

OF POOR QUALITY

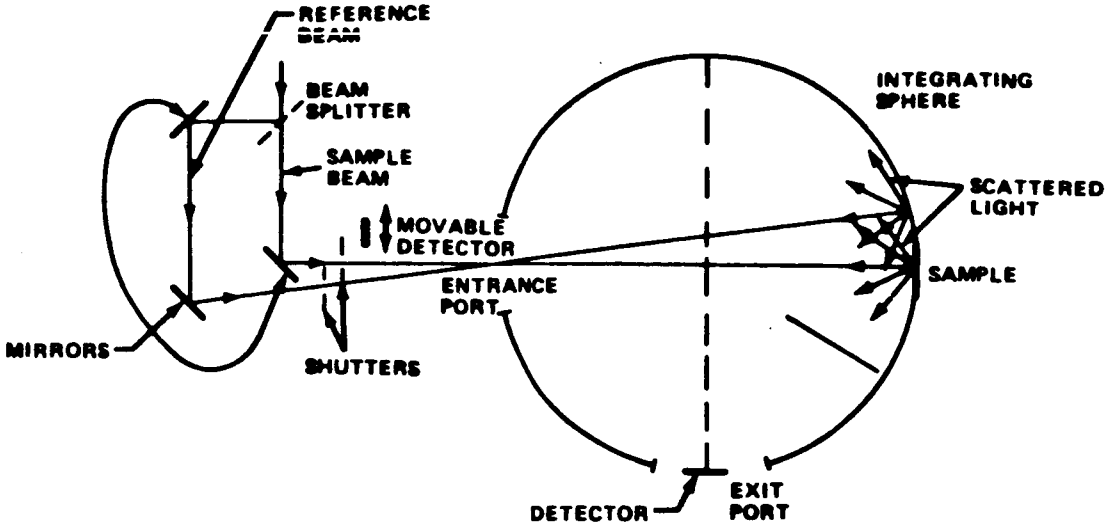

Figure 3. Dual beam measurement technique

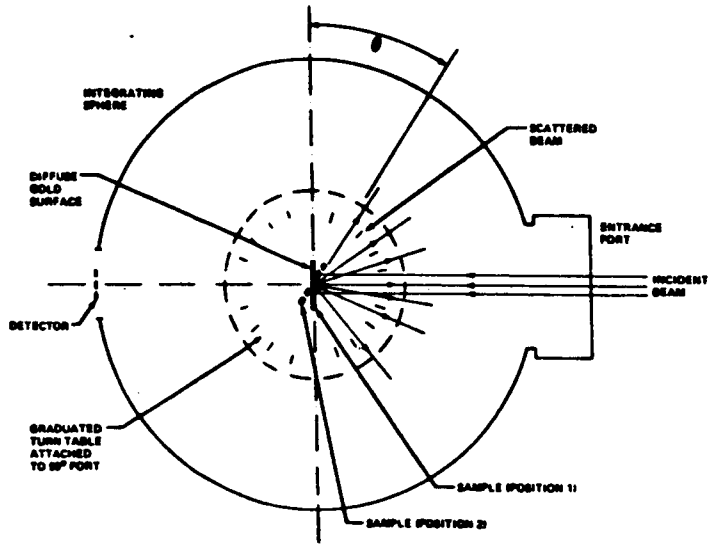

Figure 4. Edward's method

In the dual beam method the incident beam is split into two beams by a beam splitter and mirrors. One beam strikes the sample normally and is called the sample beam. The other strikes the sphere wall adjacent to the sample, so the angle of incident is small. This is called the reference beam. In the infrared using different polarizations of the incident beam the intensities will vary and must be measured before irradiating the sample or sphere. One beam and then the other is covered and the signal measured. This experimental arrangement is seen in Figure 3. The emergent flux for the irradiated wall is

$$\phi_{m_\omega} = f_m \rho_\omega \phi_{\omega_o}/\{1-\rho_\omega(1-f_e-f_m-f_s)-\rho_s f_s\}$$

$$= f_m \rho_\omega \phi_{\omega_o}/\{1-\rho_\omega\alpha_2-\rho_s f_s) \qquad (48)$$

and when the sample is irradiated, it is

$$\phi_{m_s} = f_m \rho_s \phi_{s_o}/\{1-\rho_\omega\alpha_2-\rho_s f_s\} \qquad (49)$$

Let

$$\gamma = \phi_{\omega_o}/\phi_{s_o} \qquad \text{and} \qquad \beta = S_{m_\omega}/S_{m_s} \qquad (50)$$

then

$$\rho_s(2\pi) = \rho_\omega \gamma/\beta \qquad (51)$$

The method yields a simple equation for $\rho_s(2\pi)$ but the experiment method is difficult because of the inability to properly monitor the initial fluxes.

In the Edward's method the directional-hemispherical reflectance can be measured using a single incident beam of a given polarization. The sample is mounted on a diffuse gold coated sample holder having the same reflectance as the wall. The sample holder is inserted into the center of the sphere on a graduated, rotatable table through the 90° port. This arrangement is seen in Figure 4. The reflectance of the diffuse gold coated sphere wall is measured for the appropriate CO_2 polarized radiation, so ρ_ω is well known. This is also the reflectance of the back side of the sample holder. The sample holder itself protects the detector from direct and first strike radiation as long as the angle of incidence is not too large (<60° or 70°). The detector is placed at the original sample port.

In this experiment the sample is irradiated by CO_2 laser radiation of a known wavelength and polarization in a near parallel beam with an angle of incidence θ_i and $\phi_i=0^\circ$. The signal is measured as S_{ms} . The sample is rotated in one direction through 180° and the signal from gold is measured S_{m_ω} . Using equation (51) $\gamma=1$, so

$$\rho_s = \rho_\omega/\beta \tag{52}$$

where $\beta=S_{m\omega}/S_{ms}$ and reflectances at many angles of incidence can be measured from normal to <60° or 70°.

EXPERIMENTAL PROCEDURE

In this experiment a grating tuned 7.5 W CO_2 laser was tuned to the P(24) and p(20) 10 μm lines and the R(20), R(26) and P(20) 9 μm lines. These wavelength settings were verified using a CO_2 laser spectrum analyzer. A 50/50 beamsplitter intercepted the beam, so a portion was sent to the integrating sphere and the remainder to the spectrum analyzer or to a monitoring detector. After the line was located, the detector was placed between the beamsplitters and spectrum analyzer to monitor the consistency of the laser intensity.

The reflected light from the beamsplitter was reflected into the sphere by a mirror. The initial signal was detected using a Laser Precision power meter whose analogue output was measured on a Fluke digital voltmeter. The signal was in the milliwatt level and it was required to read it to the nearest microwatt. The Laser Precision meter had drift at this level, so a more elaborate lock-in amplifier must be used in the final analysis.

The only method used this year was the substitution method, for the sphere was not modified to perform directional-hemispherical reflectance measurements by the Edward's method. The integrating sphere had to be used in an unusual manner to perform substitution measurement, for there was no baffle to protect the detector. These techniques reduced our signal levels and it could never be certain that some first strike radiation did not reach the detector. The iris diaphragm holder might reflect 3% of the first strike light into the detector. As a typical example, a 3% change in signal levels due to aperture scattering can lead to approximately a 1 to 1.5% reduction in reflectance.

The throughput of the integrating sphere is given by equation (24). For our 10" sphere with 2.75" diameter entrance and exit ports, a 1.445" sample port, and a 1 cm^2 detector element placed on the surface of the sphere, the throughput was 0.5% for a sphere reflectance, $\rho_\omega = 90\%$. This means for a 1 W input signal a 5 mW output signal is measured.

All samples have flat faces in the place of faces with the curvature of the sphere. This leads to an error

$$\varepsilon \cong r^2/4D^2 = 0.0052 \approx 0.5\%$$

This error is negligible compared to other experimental errors.

DATA AND RESULTS

The detector in an integrating sphere should be protected from incident and first strike radiation be baffle. In our sphere the baffle was in the center of the sphere between the incident and sample ports, so that sample could not be directly irradiated. The 3" baffle should instead be located as shown in Figure 7. A smaller diameter baffle could be placed nearer the detector.

Figure 5 and 6 show the illumination techniques required for uniform irradiation and normal irradiation of the sample when there is no baffle. The laser beam is nearly a parallel incident beam. If a baffle is present, the sphere wall is irradiated adjacent to the sample (Figure 1). In our case light entered the 90° port and struck the wall adjacent to the detector. In order to avoid scattered light, the detector must be moved away from the port. In our case the detector element was moved back 1-3/4" from the sphere wall outside the port. This situation is shown in Figure 5, except the detector was placed outside the iris shutter holder. In Figure 6 it is obvious that the detector must be placed at least 3" from the sphere surface. The detector position shown in the figure is 2" and first strike light still enters the detector. It is obvious that a proper baffle must incorporated in the sphere and this will greatly enhance signal levels, for then the detector can be placed at the sphere surface.

If a baffle is added to the sphere to shield the detector from incident and first strike reflected light in bihemispherical and Edward's method measurements, this will enhance the measured signal for the detector can be mounted at the sphere surface. An indication of the improvement is found by using a scale drawing of the sphere without the baffle. In bihemispherical measurements the detector is located so it can view only 53% of the sphere area and in normal incidence measurements only 21% of the sphere surface area can be viewed by the detector. With a baffle or by using the Edward's method radiation from nearly the entire sphere area can be viewed. As a result, the use of a baffle and of Edward's method is mandatory for improved signal levels.

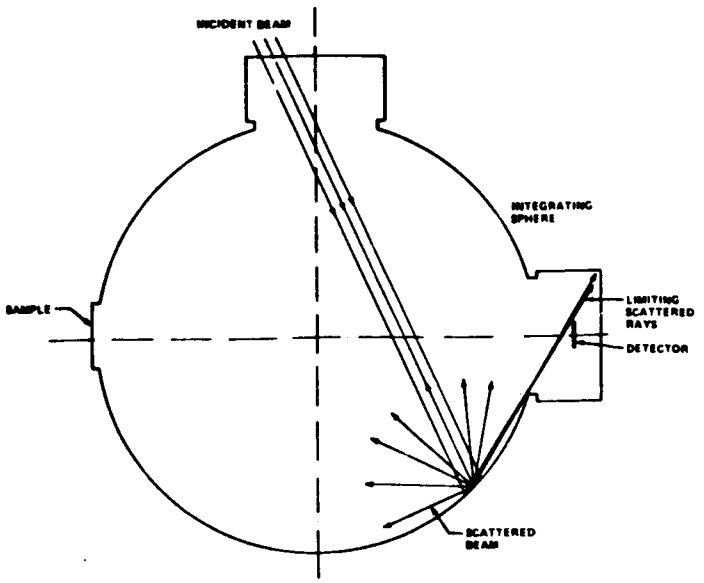

Figure 5. Uniform irradiation problem

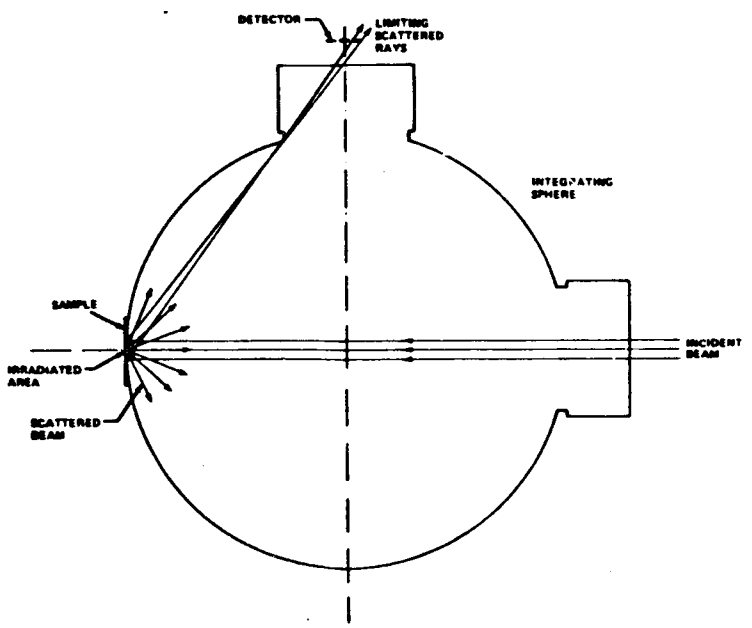

Figure 6. Direct irradiation problem

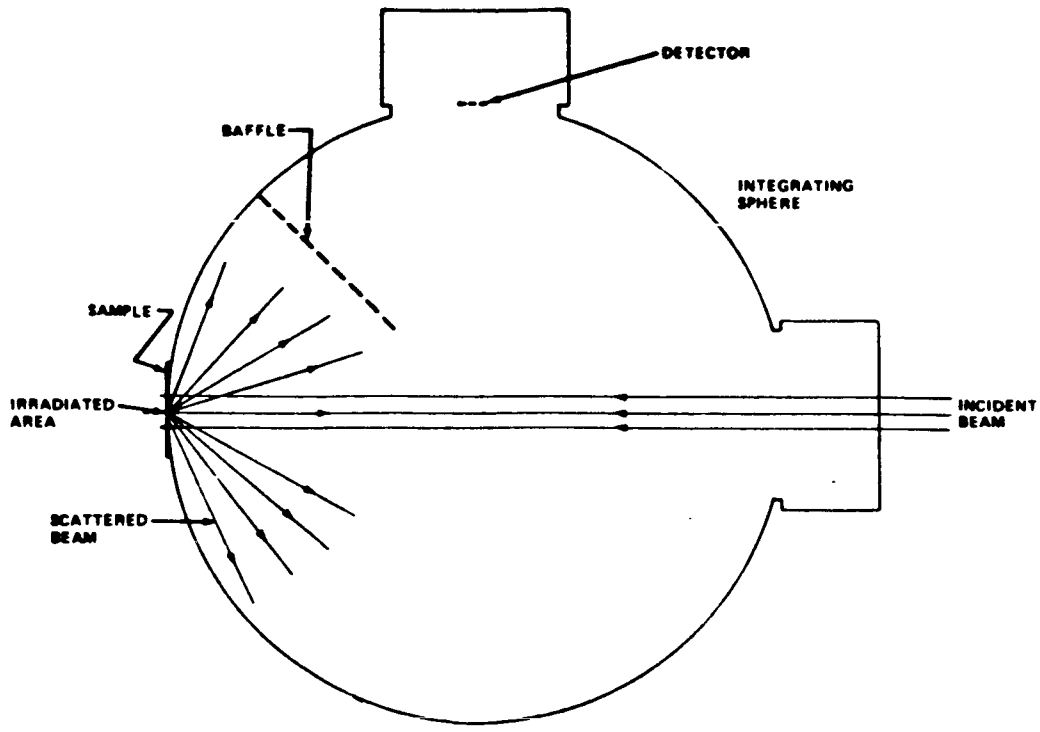

Figure 7. Correct baffle position

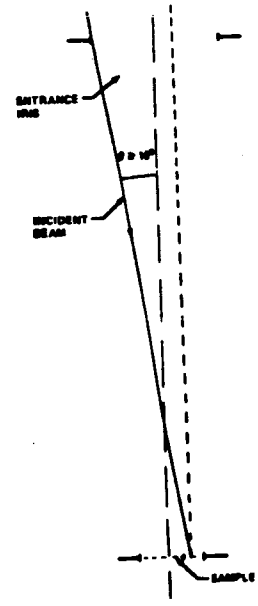

Figure 8. Small irradiation angle

Table 1 gives the results of the bihemispherical reflectance measured for the diffuse gold sample, 5-10 grit sandblasted Al, 120 grade aluminum oxide sandpaper, and flowers of sulfur. There probably is some first strike light entering the detector from the iris shutter and this could lead to reflectances 1 to 1.5% too low. The results obtained for gold, aluminum, and sulfur are satisfactory within an allowable amout of error. These reflectances were measured by the substitution technique with measurements taken with and without the sample. The gold sample was supplied by the manufacturer of the sphere and had the same reflectance as the walls.

The reflectance of the sandpaper is so small that accuracy could not be obtained with the Laser Precision detector, signals must be measured to the nearest microwatt for milliwatt signal levels. A different detection technique must be employed for low reflectance samples. The Laser Precision probe (RKP-360) is used in their most sensitive detectors and if it is combined with a chopper and PAR lock-in amplifier, signals of this order might be measured.

It should be noted that the Eppley thermopile and the room temperature HgCdTe detector are not the answer to the problem. These detector and many others have effective surface areas of $1cm^2$, so irradiance can be directly measured. Using the CO_2 laser, the greatest input into the integrating sphere at 10.6 μm is ~ 2.5W and at 9.2 μm it is ~ 1.5W. If the sphere is modified by the use of a detector baffle or the Edward's method, the detector signals would be ~13mW and ~ 7.8mW, respectively. This is based on the throughput calculation for a 1 cm^2 surface mounted detector. The sensitivity of the thermopile is 0.0965 volts/μ watt cm^2. For the 1 cm^2 thermopile the signal levels would be ~ 1.25 millvolts and ~ 0.75 millvolts, respectively. In order to evaluate surfaces with low reflectance, the signal must be measured to the nearest microvolt.

A similar problem arises for the HgCdTe detector for its responsivity is 1 to 10 millivolts/watt and signals would range from ~130 to 13 microvolts and ~ 78 to 7.8 microvolts, respectively. The amplified signal from a pyroelectric detector has the greatest potential.

Table 1. Reflectance of diffuse gold, sandblasted aluminum, 120 grade aluminum oxide sandpaper, and flowers of sulfur

CO_2 Line	Material	Polarization Horizontal	Vertical	Circular
		%	%	%
P(24) 10.632 μm	Au	92.03 ± 0.31	92.40 ± 0.36	92.28 ± 0.41
		Combined 92.24 ± 0.39		
	S	66.16 ± 0.69	68.22 ± 0.98	67.62 ± 0.87
		Combined 67.33 ± 1.21		
	Al	72.36 ± 1.87	74.59 ± 1.94	72.36 ± 1.96
		Combined 73.11 ± 2.14		
	Sandpaper	7.54 ± 1.43	8.20 ± 1.95	7.29 ± 1.69
		Combined 7.68 ± 1.72		
P(20) 10.591 μm	Au	92.05 ± 0.47	92.29 ± 0.38	92.17 ± 0.48
		Combined 92.17 ± 0.45		
	S	67.30 ± 5.18	71.20 ± 2.15	69.82 ± 0.77
		Combined 69.44 ± 3.60		
	Al	72.22 ± 1.92	73.48 ± 0.90	72.99 ± 2.71
		Combined 72.89 ± 1.49		
	Sandpaper	9.28 ± 2.60	7.78 ± 1.23	8.01 ± 2.71
		Combined 8.36 ± 2.34		
R(20) 9.271 μm	Au	89.88 ± 0.61	89.90 ± 0.71	89.87 ± 0.70
		Combined 89.87 ± 0.68		
	S	70.41 ± 8.66	69.91 ± 6.48	63.82 ± 8.78
		Combined 68.05 ± 8.47		
	Al	72.30 ± 2.47	73.62 ± 2.44	73.35 ± 2.61
		Combined 73.09 ± 2.53		
	Sandpaper	6.41 ± 2.67	6.80 ± 2.00	6.64 ± 1.84
		Combined 6.62 ± 2.17		
R(26) 9.239 μm	Au	89.32 ± 0.94	90.29 ± 0.87	90.00 ± 0.85
		Combined 89.87 ± 0.96		
	S	69.10 ± 3.57	70.55 ± 4.02	66.07 ± 2.99
		Combined 68.58 ± 3.97		
	Al	71.73 ± 3.65	74.39 ± 2.49	73.22 ± 5.16
		Combined 73.12 ± 4.01		

Table 1.

Sandpaper	6.92 ± 3.04	7.98 ± 3.07	8.99 ± 2.72
Combined	7.96 ± 3.02		

The noise level of the Laser Precision detector was checked by blocking the detector and zeroing the analogue output. The instrument was zeroed four times while the output was randomly sampled 165 times. At the analogue output a microwatt signal corresponds to measuring a tenth of a millivolt signal. The average of the 165 readings was 0.00008 + 0.00018 volt or the signal varied by 0.2 millivolts. This corresponds to power variation of ± 2 microwatts. The extreme effects of this variation on a typical signal is shown in Table 2.

Table 2. Maximum deviation in a typical reading produced by ± 2 microwatt detector signal variation

Line	Material	Typical reflectance %	Deviation produced by detector variation
P(24)	Au	92.03	± 1.02
	S	67.72	± 0.91
	Al	74.28	± 0.96
	Sandpaper	7.06	± 1.04
P(20)	Au	92.07	± 0.80
	S	69.71	± 0.84
	Al	73.22	± 0.80
	Sandpaper	7.93	± 0.93
R(20)	Au	91.13	± 2.50
	S	67.12	± 2.45
	Al	72.88	± 2.57
	Sandpaper	7.80	± 2.83
R(26)	Au	89.66	± 2.96
	S	68.35	± 1.84
	Al	77.29	± 2.57
	Sandpaper	8.57	± 2.85

The signals in Table 1 are the average of twenty measurements and some of this detector variation is averaged out, but from Table 2 if is evident that the detection system is the main contributor to the uncertainty in the measurement. This becomes extremely important for the measurement of 9 μm lines which are half the intensity of the 10 μm lines.

The reflectance of flowers of sulfur can be compared with other experiments. Kronstein and Kraushaar measured it as 92% and 86%, Blevin and Brown as 60 % and 63% and Kavaya and coworkers measured it as 66% in both the 9.2 and 10.6 μm spectral regions, respectively. Our results agreed well with Kavaya. All of these measurments used incoherent black body sources and an integrating sphere. This is the first coherent source measurment, except for the f_r measurement of Post.

The sulfur target was made by filling a cavity in a sample holder with a slurry of flowers of sulfur and acetone. The surface was made level by carefully drawing a slide across the surface. It appeared that the surface was level, but it had small ripples when hand drawn. The other samples were machined surfaces or modified machined surfaces. In the measurements of sulfur in Table 1, the sample was placed in the sphere in a random manner. In order to check the effects of surface texture it was placed in the sphere at two orientations at 90° to each other. Results for the P(24) line are given in Table 3 and the effect of sample orientation appears very small.

Table 3. The effects of sample orientation on the reflectance of sulfur

Line	Polarization	Position 1 %	Position 2 %
P(24)	Vertical	67.04 ± 1.99	66.54 ± 1.75
	Horizontal	66.90 ± 0.94	66.43 ± 1.57
	Circular	67.40 ± 1.90	67.13 ± 2.17
	Combined	67.11 ± 1.66 Combined	66.70 ± 1.84

The reflectance was remeasured for the P(24) and P(20), 10.6 μm lines, and the R(20), 9.2 μm line. The sample was inserted in position 1 in order to note any difference between a fixed sample position versus random positions. The results are seen in Table 4.

Table 4 Sulfur reflectance for three lines for fixed and random sample orientations

Line	Position	Polarization		
		Horizontal	Vertical	Circular
		%	%	%
P(24)	1	66.90 ± 0.94	67.04 ± 1.99	67.40 ± 1.90
	Random	66.16 ± 0.69	68.22 ± 0.98	67.62 ± 0.87
		Position 1 combined	67.11 ± 1.66	
		Random combined	67.33 ± 1.21	
P(20)	1	70.33 ± 1.03	71.27 ± 1.57	69.89 ± 1.72
	Random	67.30 ± 5.18	71.20 ± 2.15	69.82 ± 0.77
		Position 1 combined	70.50 ± 1.56	
		Random combined	69.44 ± 3.60	
R(20)	1	69.57 ± 2.80	68.67 ± 2.95	66.62 ± 2.37
	Random	70.41 ± 8.66	69.91 ± 6.48	63.82 ± 8.78
		Position 1 combined	68.29 ± 2.95	
		Random combined	68.05 ± 8.47	

The main conclusion that can be reached is that by positioning the sulfur sample in the same position the results are more consistent. Each individual entry in the table is the average of twenty readings and the combined data of sixty readings. The deviation is larger for random orientation, in general, but the combined average results have the same average.

It should be noted these are uniform irradiation measurements where the incident radiation is scatttered from the diffuse reflecting gold walls before striking the target. In these type of measurements the effects of polarization should be lost. The effects of coherent laser radiation should also not be apparent in the bihemispherical measurements, for phase information is also lost. The effects of polarization and coherence should become apparent in directional-hemispherical measurements.

Post and coworkers have measured the bidirectional reflectance distribution function f_r for sulfur and 120 grade aluminum oxide sandpaper at the angles $\theta_i = 45°, \phi_i = 0°, \theta_r = -45°$, and $\phi_r = 0°$ at 10.6 μm using a coherent lidar and hard scattering targets. Their values were $f_r(\text{sulfur}) = f_{rs} = 1.8 \times 10^{-1} \pm 25\%$ sr^{-1} and f_r (sandpaper) = $f_{rsd} = 1.5 \times 10 \pm 25\%$ sr^{-1}. Equation (6) relates the bidirectional reflectance distribution function and the directional-hemispherical reflectance of a surface. Using their data, the directional-hemisphere reflectances are ρ sulfur $(45°, 0°; 2\pi) = 0.80 \pm 25\%$ and ρ sandpaper $(45°, 0°; 2\pi) = 0.067 \pm 25\%$. In this study the bihemispherical reflectance was measured, but there is close agreement between values. In our experiment ρ sulfur $(2\pi, 2\pi) = 0.705 \pm 0.016$ and ρ sandpaper $(2\pi, 2\pi) = 0.084 \pm 0.023$. It must be mentioned that equation (6) holds only for a perfect diffuse scatter. (Lambertian surface) and neither sulfur or sandpaper meet this criterian.

For aluminum and sandpaper the samples were directly illuminated and these signals compared to directly illunimated gold. These measurements yield the normal incident directional- hemispherical reflectance, $\rho(2\pi)$. These results are shown in Table 5. These measurements for aluminum compared closely with our $\rho(2\pi, 2\pi)$ measurements. They are all slightly lower than the bihemispherical reflectance measurements. One could not detect any meaningful difference in reflectance with polarization. The deviation in the sandpaper measurements were much less than for the bihemispherical reflectance measurements. Again, no conclusion can be reached about a difference in reflectance with polarization of the incident light. The P(20) 9.567 μm line was also measured and the reflectance for sandpaper is lower for this line than for the P(24) and P(20) 10.6 μm lines and the R(20) 9.2 μm line. Only by measuring the reflectance of a few more lines between 10.6 and 9.2 μm will resolve this problem. It should also be noted that deviations for the low reflecting sandpaper is much smaller in the directional-hemispherical measurements than in bihemispherical measurements. The same detection equipment is used in both experiments. It appears that the uniform illumination measurements are inherently more noisy than the direct illumination measurements, though the measured signal level is greater in uniform illumination. This is an unsolved problem.

Table 5. Normal incident directional-hemispherical reflectance, $\rho(2\pi)$, of aluminum and 120 grade aluminum oxide sandpaper.

CO_2 Line	Material	Polarization Horizontal %	Vertical %	Circular %
P(24) 10.632 μm	Al	68.95 ± 0.43	69.11 ± 0.30	68.96 ± 0.39
			Combined 69.01 ± 0.38	
	Sandpaper	5.03 ± 0.18	5.24 ± 0.06	5.20 ± 0.09
			Combined 5.24 ± 0.06	
P(20) 10.591 μm	Al	71.28 ± 0.50	71.53 ± 0.51	71.06 ± 0.44
			Combined 71.31 ± 0.52	
	Sandpaper	5.16 ± 0.08	5.73 ± 0.06	5.33 ± 0.08
			Combined 5.41 ± 0.25	
P(20) 9.567 μm	Al	67.89 ± 0.27	68.08 ± 0.47	68.00 ± 0.93
			Combined 67.99 ± 0.62	
	Sandpaper	4.24 ± 0.08	4.22 ± 0.06	4.22 ± 0.15
			Combined 4.22 ± 0.10	
R(20) 9.271 μm	Al	68.44 ± 0.45	68.36 ± 0.33	68.20 ± 0.37
			Combined 68.33 ± 0.39	
	Sandpaper	5.35 ± 0.13	5.36 ± 0.12	5.38 ± 0.15
			Combined 5.36 ± 0.13	

In table 6 the reflectance of the gold coating are compared. It appears that the reflectance decreases from the 10.6 to the 9.2 μm regions. One would expect a near uniform reflectance and this problem must be re-examimed with the modified apparatus.

Table 6. Summary of diffuse gold wall coating reflectance.

CO_2 Line	Polarization Horizontal %	Vertical %	Circular %
P(24) 10.632 μm	92.03 ± 0.31	92.40 ± 0.36	92.28 ± 0.41
		Combined 92.24 ± 0.39	
P(20) 10.591 μm	92.05 ± 0.47	92.29 ± 0.38	92.17 ± 0.48
		Combined 92.17 ± 0.45	
P(20) 9.567 μm	90.44 ± 1.15	90.79 ± 0.92	89.85 ± 0.70
		Combined 90.35 ± 1.12	
R(20) 9.271 μm	89.88 ± 0.61	89.90 ± 0.71	89.87 ± 0.70
		Combined 89.87 ± 0.68	
R(26) 9.239 μm	89.32 ± 0.94	90.29 ± 0.87	90.00 ± 0.85
		Combined 89.87 ± 0.96	

Figure 8 shows that the sample can only be irradiated through very small angles. If extensive and meaningful directional-hemispherical reflectance are to be measured, the Edward's technique must be used. This method was described earlier and is shown in Figure 4. The sphere will require extensive modification to mount the rotatable table on the 90° port. This modification must also be removeable, so the substitution method can be used to measure the bihemispherical reflectance and the wall reflectance. The rotatable mount must have a very small reflectivity in the port region, so the ρ of the port area may be taken as zero. The sample holder components which are placed inside the sphere must be sent to the sphere manufacturer to be coated with a diffuse gold coating like the sphere wall.

The dual beam technique would pose problems in the infrared because of the multiple reflections and the various polarization of the radiation. The losses would be large, the two beams would be of different intensity and an accurate detector would have the monitor both beams to measure ϕ.

CONCLUSIONS AND RECOMMENDATIONS

The conclusions are that both bihemispherical and directional-hemispherical reflectance can be measured versus polarization for CO_2 laser lines. Bihemispherical measurements were performed on three samples and a diffuse gold coated sample with a coating similar to the sphere to measure ρ_ω. Even though an unusual geometry was required since the cell had no baffle, satisfactory results were obtained for all specimens with high reflectance. This geometry resulted in a serious loss of intensity and a small amount of first strike light may have entered the detector so the readings may be 1 to 1.5% too low. In order to measure low reflectance, which is represented by sandpaper, the signal must be measured accurately to the microwatt level for signal in the milliwatt range. Thus, improved detection techniques must be found. A few normal incident directional-hemispherical measurements have been made for aluminum and sandpaper.

Several recommendations are made and are the following: (1) the placement of a baffle in the sphere to shade the detector from first strike light; (2) improve the detection techniques by the use of a modified Laser Precision probe detector, chopper, and PAR lock-in amplifier or the use of heterodyne detection techniques, (3) the mounting of the detector in the port at the region on the sphere wall to reduce signal loss; (4) the modification of the integrating sphere so the sample can be mounted at the sphere center on a diffuse gold coated mount which is attached to graduated, rotatable table and the system is installed through the 90° port; (5) improved cooling of the CO_2 laser to improve intensity stabilization; and (6) the purchase of additional diffuse gold coated samples with a gold coating like the sphere for they are used extensively and may become damaged in time.

After these modification are complete the following experiments are suggested; (1) gold wall coating reflectance should be measured from 10.6 μm to 9.2 μm at six CO_2 lines to ascertain if the reflectance actually decreases; (2) the number of samples under study should be increased and might include plasma deposited surface, black glass bead targets, liquid steel and aluminum surfaces, etc; (3) the bihemispherical reflectance should be measured for these samples; and (4) the directional-hemispherical reflectance shoud be measured for the samples at several incident angles between 0°and 60° or 70°.

REFERENCES

1. Rothermal, J. and Jones, W.D., "Ground-base measurements of atmospheric backscatter and absorption using coherent CO_2 lidar," Applied Optics 24, 3487-3496 (1985)

2. Kavaya, M.J., Menzies, R.T., Haner, D.A., Oppenheim, U.P., and Flamont, P.H., "Target reflectance measurements for the calibration of lidar atmospheric backscatter data," Applied Optics 22, 2619-2628 (1983)

3. Kavaya, M.J., and Menzies, R.T., "Aerosol backscatter lidar calibration and data interpretion," J.P.L. Publication 84-6, National Aeronautics and Space Administration, March 1, 1984.

4. Nicodemas, F.E., Richmond, J.C., Ginsberg, I.W., and Limperis, T.,"Geometrical considerations and nomenclature for reflectance," National Bureau of Standards Mongraph 160, Oct. 1977.

5. Lovell, J.,"Integrating sphere performance," Labsphere, North Sutton, New Hampshire (1981)

6. Goebel, D.G., "Integrating-sphere theory" Applied Optics, 6, 125-128 (1967)

7. Jacquez, J. A. and Kuppenheim, H. F., "Theory of integrating spheres," Journal Optical Society of America 45, 460-470 (1955)

8. Edwards, D.K., Grier, J.T., Nelson, K.E., and Roddick, R.D., "Integrating sphere for imperfectly diffusing samples," Journal Optical Society of America 51, 1279-1288 (1961)

9. Miller, O.E., and Sant, A. J., "Incomplete integrating sphere", Journal Optical Society Of America 48, 828-831 (1958)

10. Venable,W.H., Jr, Hsia, J.J., and Weidner, V.R., "Development of an National Bureau of Standards spectrophotometer for diffuse transmittance and reflectance ", National Bureau of Standards Technical Note, 594-611 (1976)

11. Laser Precision Corp. private communication.

12. Kronstein, M. and Kraushaar, R.J., "Sulfur as a standard of reflectance in the infrared", Journal of Optical Society of America 53, 458-465 (1963)

13. Blevin, W.R and Brown, W.J., "An infrared reflectrometer with a spherical mirror", Journal of Scientific Instruments 42, 385-389 (1965)

14. Post, M.J., Richter, R. A., Keeler, R.J., Hardesty, R.M., Lawrence, T.R., and Hall,F.F., "Calibration of coherent lidar targets", Applied Optics 19, 2828-2832 (1980)